Baghdad Science Journal

Volume 23 | Issue 6 Article 20

6-22-2026

Numerical Study of the Effect of Embedded Radiation on Fluid Flow and Heat Transfer in a Porous Medium

Shaymaa M. Younus
Department of Mathematics, College of Education for Pure Science, University of Mosul, Mosul, Iraq, Shaymaa.mohammed@uomosul.edu.iq

Iman Al-Obaidi
Department of Mathematics, College of Education for Pure Science, University of Mosul, Mosul, Iraq, emanhashem1986@uomosul.edu.iq

How to Cite this Article

Younus, Shaymaa M. and Al-Obaidi, Iman (2026) "Numerical Study of the Effect of Embedded Radiation on Fluid Flow and Heat Transfer in a Porous Medium," *Baghdad Science Journal*: Vol. 23: Iss. 6, Article 20.
DOI: https://doi.org/10.21123/2411-7986.5334

BAGHDAD SCIENCE JOURNAL 2026;23(6):2206–2215

RESEARCH ARTICLE

Numerical Study of the Effect of Embedded Radiation on Fluid Flow and Heat Transfer in a Porous Medium

Shaymaa M. Younus, Iman Al-Obaidi *

Department of Mathematics, College of Education for Pure Science, University of Mosul, Mosul, Iraq

ABSTRACT

This takes a look at ambitions to investigate the two-dimensional flow pattern of fluids in a conductive medium constrained between two parallel horizontal plates under the influence of embedded radiation. The mathematical model is based entirely on the flow equations, including the continuity, momentum, energy, and diffusion equations. The machine is solved numerically the usage of the specific finite difference approach (ADE) to investigate the conduct of drift, temperature, and mass transfer below radiative outcomes. The study specializes in the impact of key dimensionless parameters, including the Reynolds number, Darcy number, Grashof number, Péclet number, radiation parameter, mixed radiation, and thermal absorption coefficient, on temperature and concentration distributions within the porous medium. The effects indicate that growing the combined radiation complements the temperature in the porous layer, while the Darcy range considerably influences the fluid velocity and balance. MATLAB program software became employed to perform the numerical analysis and visualize the outcomes, imparting a clear understanding of the float flow conduct and heat and mass transfer in porous media under thermal radiation conditions. The significance of this study lies in clarifying the role of thermal radiation in modifying and enhancing the heat transfer characteristics within porous.

Keywords: Alternative direction explicit method, Darcy number, Embedded radiation, Radiation parameter, Thermal absorption coefficient

Introduction

Fluid mechanics is a branch of applied mechanics that studies the motion and formation of fluids. The study of fluid flow is a fundamental field in engineering and the physical sciences, as it plays a vital role in understanding the behavior of materials under various dynamic conditions. [1] Sarojamma, Sreelakshmi, and Animasaun studied the motion of a low-viscosity fluid in a magnetodynamic state in the presence of thermal radiation using the Range-Kutta method. [2] Abu Zeid, Shaalan, and Raslan presented a numerical solution to the B-Spling function to explain how both mass and heat are spread over an unsteady fluid flow according to the proposed model. [3] Liu, Jiang, and Chong adopted a numerical approach to solve the problem of heat diffusion of a fluid within a permeable medium, and through this, they demonstrated the effect of wall thickness. [4] Feng, Liu, and He, Y. L. Heat diffusion in porous media on the REV scale was studied using the lattice Boltzmann method (CLB) and numerically obtained stable parameters. [5] Asjad et al. presented an analytical study using Laplace transforms for the flow of an incompressible viscous fluid through a porous medium under the influence of magnetic forces, employing a hybrid fractional derivative with constant proportionality. [6] Hammodat, Algwauish, and

Received 24 September 2025; revised 30 December 2025; accepted 16 March 2026.
Available online 22 June 2026

* Corresponding author.
E-mail addresses: Shaymaa.mohammed@uomosul.edu.iq (S. M. Younus), emanhashem1986@uomosul.edu.iq (I. Al-Obaidi).

https://doi.org/10.21123/2411-7986.5334

Al-Obaidi dealt with a mathematical problem of fluid flow between two parallel plates with porous walls under the influence of a magnetic field, and through it, the properties of the fluid were studied in terms of speed and temperature.[7] Danish et al. considered an unsteady Williamson fluid to investigate heat and mass transfer in a magnetohydrodynamic (MHD) environment under the influence of externally generated thermal radiation forces. Through this study, the effects of the resulting physical parameters were analyzed and interpreted.[8] Ikram et al. have used nanotechnology to solve the problem of heat diffusion in some engineering and industrial applications by performing multiplicative calculus on a nanofluid.[9]

Rafee and Saddam studied numerically a model consisting of a plate placed vertically inside a porous medium in the presence of a radiation source using the (F.D.M) method.[10] Rahaman et al. discovered a solution to the water pollution problem by formulating a mathematical model based on the one-dimensional convection and diffusion equations and solving it numerically using the ADE method, while imposing appropriate initial and boundary conditions for the model.[11] Ahmed et al.The bvp4c) algorithm was employed to conduct a numerical study of a nanofluid under the influence of a magnetic field, and the results revealed an inverse relationship between the fluid velocity and the magnetic field intensity.[12] Abbas et al. proved that the change in density affects the flow of gray fluid, by using a numerical method in a magnetic environment.[13] Al-Khafajy et al. studied how both thermal radiation and the Lorentz force affect a vertical plate in terms of speed and temperature, relying on the finite difference method.[14] Chouderley explains the relationship between increased radiation and decreased temperature using the turbulence technique, while explaining the role of external forces on the fluid.[15] Saleem revealed, based on a numerical study of a mathematical model, several physical parameters that directly impact heat transfer in fluid flow in horizontal and inclined channels.[16] Kumar et al. used the fourth-order Runge-Kutta method, along with an optimization approach, to approximate the results. Some non-dimensional parameters were observed to have adverse effects on the fluid flow under the influence of thermal radiation.[17] In this research, the explicit specific differences (ADE) method was adopted to demonstrate the effect of integrated radiation and temperature distribution on the fluid flow behavior within a porous medium. Through this method, the dynamic response of the fluid in this field was evaluated, and several parameters affecting this flow were identified; their effects on the model were illustrated using graphical representations.

Model of mathematics and fundamental equations

Fig. 1 illustrates the problem of heat and mass transfer in a steady fluid within a two-dimensional porous medium in the Cartesian coordinate system. The fluid is confined between two parallel horizontal plates, with the upper wall thermally insulated ($\frac{\partial \hat{T}}{\partial \hat{y}} = 0$), preventing the passage of materials and being exposed to incident thermal radiation. The lower wall is heated at a constant temperature ($\hat{T} = \hat{T}_w$) and concentration ($\hat{c} = \widehat{c_0}$). The fluid is assumed to flow from the left edge at zero initial temperature and concentration and zero velocity, and to exit from the right side under normal flow conditions. Furthermore, the filled medium is assumed to be equally porous and subject to fluid and mass movement under the influence of radiation, convection, and diffusion.

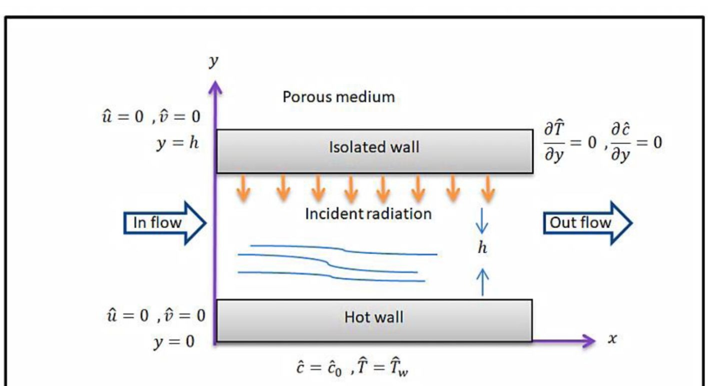

Fig. 1. Model of mathematics.

The following are the basic dimensional differential equations that govern the problem:-
The equation of continuity

$$\frac{\partial \hat{u}}{\partial x} + \frac{\partial \hat{v}}{\partial y} = 0 \tag{1}$$

Equation of motion x & y directions

$$\rho\left(\hat{u}\frac{\partial \hat{u}}{\partial x} + \hat{v}\frac{\partial \hat{u}}{\partial y}\right) = -\frac{\partial \hat{p}}{\partial x} + \mu_{eff}\left(\frac{\partial^2 \hat{u}}{\partial x^2} + \frac{\partial^2 \hat{u}}{\partial y^2}\right) - \frac{\mu}{k}\hat{u} \tag{2}$$

$$\rho\left(\hat{u}\frac{\partial \hat{v}}{\partial x} + \hat{v}\frac{\partial \hat{v}}{\partial y}\right) = -\frac{\partial \hat{p}}{\partial \hat{y}} + \mu_{eff}\left(\frac{\partial^2 \hat{v}}{\partial x^2} + \frac{\partial^2 \hat{v}}{\partial y^2}\right) - \frac{\mu}{k}\hat{v} + \rho g \beta_T\left(\hat{T} - \hat{T}_\infty\right) + \rho g \beta_C\left(\hat{c} - \hat{c}_\circ\right) \tag{3}$$

After differentiating Eqs. (2) and (3) w.r.t x and y respectively, subtracting Eq. (2) from Eq. (3), we obtain the equation of motion in the general (dimensional) case:

$$\frac{\partial}{\partial x}\left(\hat{u}\frac{\partial \hat{v}}{\partial x} + \hat{v}\frac{\partial \hat{v}}{\partial y}\right) - \frac{\partial}{\partial y}\left(\hat{u}\frac{\partial \hat{u}}{\partial x} + \hat{v}\frac{\partial \hat{u}}{\partial y}\right) = \frac{\mu_{eff}}{\rho}\nabla^2\left(\frac{\partial \hat{v}}{\partial x} - \frac{\partial \hat{u}}{\partial y}\right) - \frac{\mu}{\rho k}\left(\frac{\partial \hat{v}}{\partial x} - \frac{\partial \hat{u}}{\partial y}\right) + \rho g \beta_T\frac{\partial \hat{T}}{\partial x} + \rho g \beta_C\frac{\partial \hat{c}}{\partial x} \tag{4}$$

$$\hat{u}\frac{\partial \hat{T}}{\partial x} + \hat{v}\frac{\partial \hat{T}}{\partial y} = \alpha\left(\frac{\partial^2 \hat{T}}{\partial x^2} + \frac{\partial^2 \hat{T}}{\partial y^2}\right) - \frac{1}{\rho C_p}\frac{\partial \hat{q}_r}{\partial y} - \frac{\hat{Q}_r}{\rho C_p} \tag{5}$$

Using Roseland's approximations for thermal radiation, which is expressed as follows. [18,19]

$$\frac{\partial \hat{q}_r}{\partial y} = -\frac{16\sigma \hat{T}_\infty^3 \propto}{3k^*}\frac{\partial^2 \hat{T}}{\partial y^2} \tag{6}$$

By substituting Eq. (6) into Eq. (5), the energy equation becomes as follows:
Energy equation

$$\hat{u}\frac{\partial \hat{T}}{\partial x} + \hat{v}\frac{\partial \hat{T}}{\partial y} = \alpha\left(\frac{\partial^2 \hat{T}}{\partial x^2} + \left(1 + \frac{16\rho \hat{T}_\infty^3}{3k^* k}\right)\frac{\partial^2 \hat{T}}{\partial y^2}\right) - \frac{\hat{Q}_r}{\rho C_p} \tag{7}$$

Diffusion equation

$$\hat{u}\frac{\partial \hat{c}}{\partial x} + \hat{v}\frac{\partial \hat{c}}{\partial y} = D\left(\frac{\partial^2 \hat{c}}{\partial x^2} + \frac{\partial^2 \hat{c}}{\partial y^2}\right) \tag{8}$$

where velocity components are $\hat{u}$ and $\hat{v}$ represent the along the x- and y-axes respectively, ρ density, μ viscosity, μ_{eff} effective viscosity, k represents the permeability of the porous medium, $\hat{T}$ temperature, C_p specific heat capacity of a fluid at a given pressure, α thermal diffusion coefficient, $\hat{c}$ concentration, D mass diffusion, β_T and β_C Coefficient of expansion for both temperature and concentration, and $\hat{p}$ pressure.
The corresponding initial and boundary situations are:

$$\left.\begin{array}{r} \hat{u} = \hat{v} = 0 \; and \; \hat{c} = \hat{c}_0, \; \hat{T} = \hat{T}_w \quad at \; y = 0 \\ \hat{u} = \hat{v} = 0 \; and \; \frac{\partial \hat{c}}{\partial y} = 0, \; \frac{\partial \hat{T}}{\partial y} = 0 \quad at \; y = h \end{array}\right\} \tag{9}$$

Dimensional analysis

Converting the governing Eqs. (1), (4), (7) and (8) to the dimensionless state is necessary to study the model and find numerical solutions under the initial conditions indicated in Eq. (9). To obtain the dimensionless equations, the following dimensionless quantities are imposed:

$$\left.\begin{array}{c} u^* = \dfrac{\hat{u}}{U_0},\ v^* = \dfrac{\hat{v}}{U_0},\ c^* = \dfrac{\widehat{c}}{\hat{C}_0},\ p^* = \dfrac{\hat{p}}{\rho U_0^2} \\ x^* = \dfrac{\hat{x}}{h},\ y^* = \dfrac{\hat{y}}{h},\ \theta = \dfrac{\hat{T} - \hat{T}_\infty}{\hat{T}_w - \hat{T}_\infty} \end{array}\right\} \tag{10}$$

By substituting the given assumptions into Eq. (10) in Eqs. (1), (4), (7) and (8), we get:

$$\frac{\partial u^*}{\partial x^*} + \frac{\partial v^*}{\partial y^*} = 0 \tag{11}$$

$$\begin{aligned} &\frac{\partial}{\partial x^*}\left(u^*\frac{\partial v^*}{\partial x^*} - v^*\frac{\partial v^*}{\partial y^*}\right) - \frac{\partial}{\partial y^*}\left(u^*\frac{\partial u^*}{\partial x^*} - v^*\frac{\partial u^*}{\partial y^*}\right) = \frac{1}{Re}\nabla^2\left(\frac{\partial v^*}{\partial x^*} - \frac{\partial u^*}{\partial y^*}\right) - \frac{1}{ReDa}\left(\frac{\partial v^*}{\partial x^*} - \frac{\partial u^*}{\partial y^*}\right) \\ &\quad + Gr_T\frac{\partial \theta}{\partial x^*} + Gr_c\frac{\partial c^*}{\partial x^*} \end{aligned} \tag{12}$$

$$u^*\frac{\partial \theta}{\partial x^*} + v^*\frac{\partial \theta}{\partial y^*} = \frac{1}{Pe}\left(\frac{\partial^2 \theta}{\partial x^{*2}} + (1 + 4Rd)\frac{\partial^2 \theta}{\partial y^{*2}}\right) - Q^* e^{-\gamma^* y^*} \tag{13}$$

$$u^*\frac{\partial c^*}{\partial x^*} + v^*\frac{\partial c^*}{\partial y^*} = \frac{1}{Sc}\left(\frac{\partial^2 c^*}{\partial x^{*2}} + \frac{\partial^2 c^*}{\partial y^{*2}}\right) \tag{14}$$

Where $Re, Da, Gr_T, Gr_c, Rd, Pe, Sc, Q^*$ and γ^* represent respectively Reynolds number, Darcy number, Grashof number for heat transfer, Grashof number for mass transfer, radiation parameter, Pécletnumber, Schmidt number, Embedded Radiation, and Thermal absorption coefficient, respectively.[20]

The resulting boundary conditions are:

$$\left.\begin{array}{c} u^* = 0, v^* = 0,\ \theta = 1, \\ c^* = 1, \dfrac{\partial \theta}{\partial y^*} = 0, \dfrac{\partial c^*}{\partial y^*} = 0 \end{array}\right\} at\ y^* = 0, y^* = 1. \tag{15}$$

Using the stream function,[21] assuming $u^* = \frac{\partial \Psi^*}{\partial y^*}$, $v^* = -\frac{\partial \Psi^*}{\partial x^*}$ and substituting $\varpi^* = \nabla^{*^2}\Psi^*$ into Eqs. (11) to (14), obtain the equations in the dimensionless case under the influence of the flow function:

$$\frac{\partial^2 \Psi^*}{\partial x^{*2}} + \frac{\partial^2 \Psi^*}{\partial y^{*2}} = \varpi^* \tag{16}$$

$$\begin{aligned} &\frac{\partial}{\partial x^*}\left(-\frac{\partial \Psi^*}{\partial y^*}\cdot\frac{\partial^2 \Psi^*}{\partial x^{*2}} + \frac{\partial \Psi^*}{\partial x^*}\cdot\frac{\partial^2 \Psi^*}{\partial x^* y^*}\right) + \frac{\partial}{\partial y^*}\left(\frac{\partial \Psi^*}{\partial y^*}\cdot\frac{\partial^2 \Psi^*}{\partial x^* y^*} - \frac{\partial \Psi^*}{\partial x^*}\cdot\frac{\partial^2 \Psi^*}{\partial y^{*2}}\right) \\ &\quad = \frac{1}{Re}\cdot\nabla^2\Psi^* + \frac{1}{ReDa}\cdot\nabla^2\Psi^* + Gr_T\frac{\partial \theta}{\partial x^*} + \cdots + Gr_c\frac{\partial c^*}{\partial x^*} \end{aligned} \tag{17}$$

$$\frac{\partial \Psi^*}{\partial y^*}\cdot\frac{\partial \theta}{\partial x^*} - \frac{\partial \Psi^*}{\partial x^*}\cdot\frac{\partial \theta}{\partial y^*} = \frac{1}{Pe}\left(\frac{\partial^2 \theta}{\partial x^{*2}} + (1 + 4Rd)\frac{\partial^2 \theta}{\partial y^{*2}}\right) - Q^* e^{-\gamma^* y^*} \tag{18}$$

$$\frac{\partial \Psi^*}{\partial y^*}\cdot\frac{\partial c^*}{\partial x^*} - \frac{\partial \Psi^*}{\partial x^*}\cdot\frac{\partial c^*}{\partial y^*} = \frac{1}{Sc}\left(\frac{\partial^2 c^*}{\partial x^{*2}} + \frac{\partial^2 c^*}{\partial y^{*2}}\right) \tag{19}$$

The resulting boundary conditions are:

$$\left.\begin{array}{c} \Psi^* = 0,\ \varpi^* = \dfrac{\partial^2 \Psi^*}{\partial y^{*2}},\ \theta = 1, \\ c^* = 1,\ \dfrac{\partial \theta}{\partial y^*} = 0, \dfrac{\partial c^*}{\partial y^*} = 0 \end{array}\right\} at\ y^* = 0, y^* = 1. \tag{20}$$

Numerical solution

Using the explicit finite-difference method and the boundary conditions imposed in the mathematical model, a system of non-linear, non-intransitive partial differential equations was obtained that describes the diffusion of mass & heat in a steady two-dimensional fluid flow in a porous environment. The flow field was divided into lines perpendicular to the x- and y-axes, where the x-axis represents the fluid flow, while the y-axis represents the distance between the two plates. Assume that the maximum value is 25, meaning that the y values range between 0 and 25, and assume that the flow field length measurements range between 0 and 100. Thus, a regular two-dimensional computer network was formed in the x- and y-directions, respectively. The P.D.E (16)–(19) with the cond. (20) was solved by FDM,[22] after assuming that m = 250 and n = 250, as well as $\Delta x^* = 0.4\ s.t\ x^* \in [0, 100]$ & $\Delta y^* = 0.4\ y^* \in [0, 25]$ as follows:

$$\frac{\Psi^*{}_{i+1,j} - 2\Psi^*{}_{i,j} + \Psi^*{}_{i-1,j}}{(\Delta x^*)^2} + \frac{\Psi^*{}_{i,j+1} - 2\Psi^*{}_{i,j} + \Psi^*{}_{i,j-1}}{(\Delta y^*)^2} = \varpi^*_{i,j} \tag{21}$$

$$\begin{aligned}&\left(\frac{\Psi^*{}_{i,j+1} - \Psi^*{}_{i,j}}{\Delta y^*} \cdot \frac{\varpi^*{}_{i,j} - \varpi^*_{i-1,j}}{\Delta x^*}\right) - \left(\frac{\Psi^*{}_{i,j} - \Psi^*_{i-1,j}}{\Delta x^*} \cdot \frac{\varpi^*{}_{i,j+1} - \varpi^*_{i,j}}{\Delta y^*}\right)\\ &\quad = \frac{1}{Re}\left(\frac{\varpi^*{}_{i+1,j} - 2\varpi^*{}_{i,j} + \varpi^*{}_{i-1,j}}{(\Delta x^*)^2} + \frac{\varpi^*{}_{i,j+1} - 2\varpi^*{}_{i,j} + \varpi^*{}_{i,j-1}}{(\Delta y^*)^2}\right)\\ &\quad - \frac{1}{ReDa}\varpi^*_{i,j} \cdots + Gr_T\left(\frac{\theta_{i,j} - \theta_{i-1,j}}{\Delta x^*}\right) + Gr_c\left(\frac{c^*_{i,j} - c^*_{i-1,j}}{\Delta x^*}\right)\end{aligned} \tag{22}$$

$$\begin{aligned}&\left(\frac{\Psi^*{}_{i,j+1} - \Psi^*{}_{i,j}}{\Delta y^*}\right)\left(\frac{\theta_{i,j} - \theta_{i-1,j}}{\Delta x^*}\right) - \left(\frac{\Psi^*{}_{i,j} - \Psi^*_{i-1,j}}{\Delta x^*}\right)\left(\frac{\theta_{i,j+1} - \theta_{i,j}}{\Delta y^*}\right)\\ &\quad = \frac{1}{Pe}\left(\frac{\theta_{i+1,j} - 2\theta_{i,j} + \theta_{i-1,j}}{(\Delta x^*)^2} + (1 + 4Rd)\frac{\theta_{i,j+1} - 2\theta_{i,j} + \theta_{i,j-1}}{(\Delta y^*)^2}\right) + Q^* e^{-\gamma^* y^*}\end{aligned} \tag{23}$$

$$\begin{aligned}&\left(\frac{\Psi^*{}_{i,j+1} - \Psi^*{}_{i,j}}{\Delta y^*}\right)\left(\frac{c^*_{i,j} - c^*_{i-1,j}}{\Delta x^*}\right) - \left(\frac{\Psi^*{}_{i,j} - \Psi^*_{i-1,j}}{\Delta x^*}\right)\left(\frac{c^*_{i,j+1} - c^*_{i,j}}{\Delta y^*}\right)\\ &\quad = \frac{1}{Sc}\left(\frac{c^*{}_{i+1,j} - 2c^*{}_{i,j} + c^*{}_{i-1,j}}{(\Delta x^*)^2} + \frac{c^*{}_{i,j+1} - 2c^*{}_{i,j} + c^*{}_{i,j-1}}{(\Delta y^*)^2}\right).\end{aligned} \tag{24}$$

Results and discussion

In this section, review the numerical solutions for a fluid that is stable inside a porous environment between two horizontal plates influenced by embedded Radiation. The explicit finite difference method (ADE) was used to obtain the numerical results and represent them graphically, using MATLAB, to deduce the numerical results, and to illustrate the drawings of the differential equations represented by Eqs. (22) to (24) as shown in Figs. 2

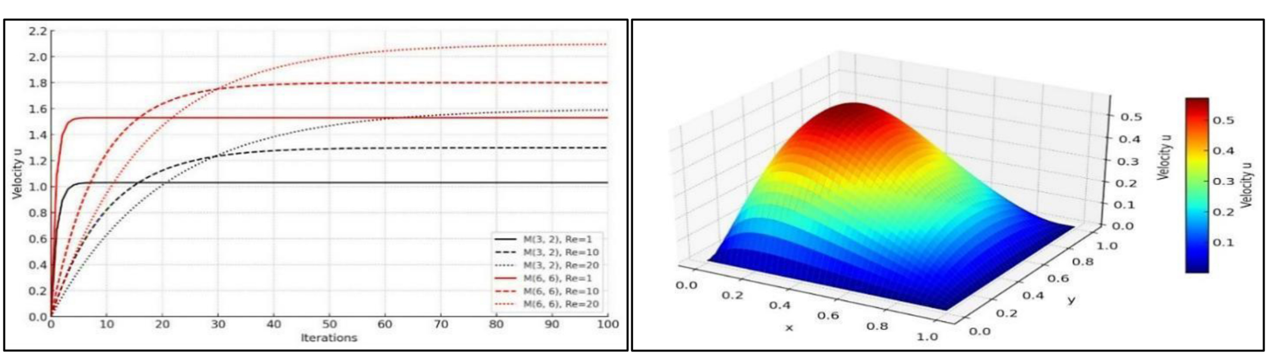

Fig. 2. Effect of Re. On the motion equation Re = (1–20), with a 3D. at Re = 20.

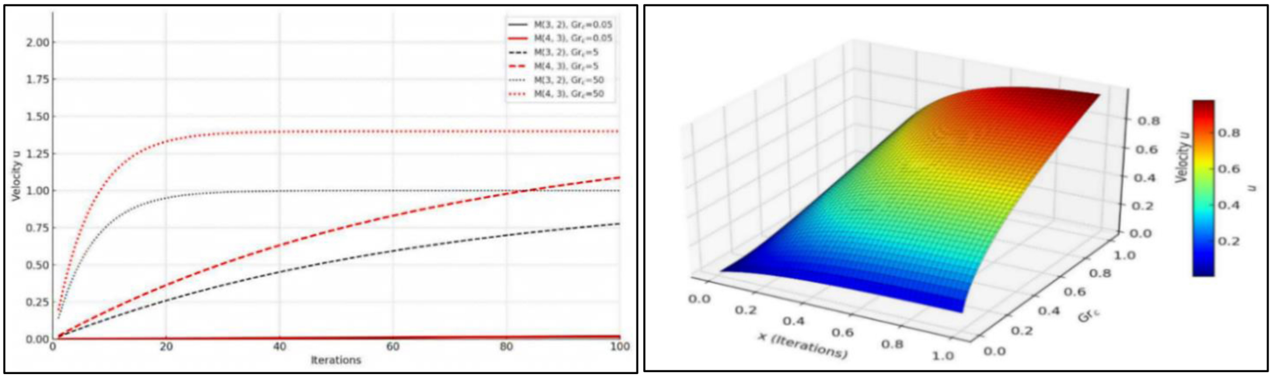

Fig. 3. Effects of $\boldsymbol{Gr_c}$ On the motion equation $Gr_c = (0.05 - 50)$, with a 3D. at $Gr_c = 5$.

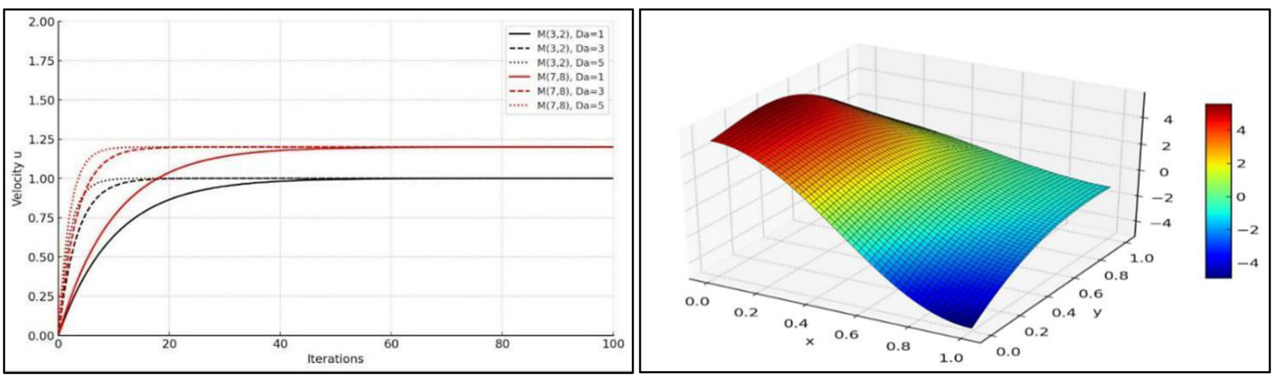

Fig. 4. Effects of Da On the motion equation $\mathrm{Da} = (1 - 5)$ with a 3D. at $\mathrm{Da} = 1.5$.

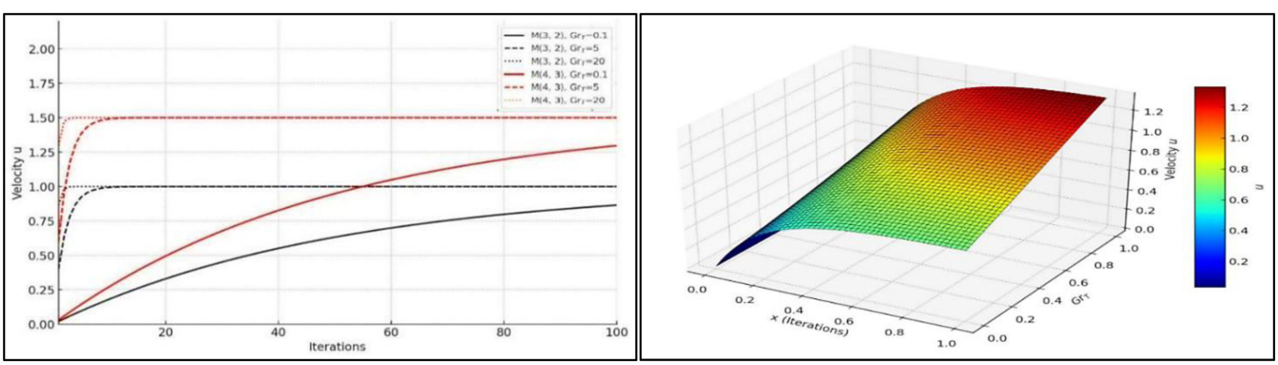

Fig. 5. Effects of Gr_T. On the motion equation $Gr_T = (0.1 - 20)$ with a 3D. at $Gr_T = 2$.

to 10. The effect of the parameters in the equation of motion is shown in Figs. 2 to 5, where it was noted in Figs. 2 and 3 that the lower the values of the Reynolds number Re and the Grashof number for mass transfer Gr_c, the more stable the system becomes.

While the effect of Darcy number Da and Grashof number for heat transfer Gr_T is shown in Figs. 4 and 5. Note that the higher their values, the closer to stability.

The parameters of the energy equation are shown in Figs. 6 to 9. In Figs. 6 and 7, the higher the values of the Pécletnumber Pe and the Embedded Radiation Q^*, the less stable the system becomes

Figs. 8 and 9 show the effect of both the Radiation parameter Rd and the thermal absorption coefficient γ^* respectively, where higher values indicate greater system stability.

Fig. 10 shows the effect of the Schmidt number Sc parameter in the diffusion equation, where the lower its value, the less stable the system becomes.

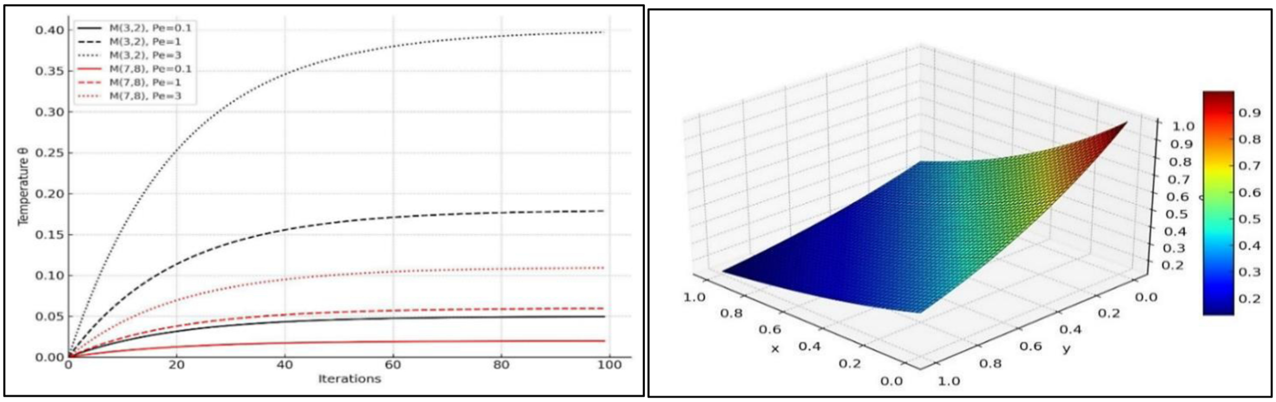

Fig. 6. Effect of the Pe. On the energy equation $Pe = (0.1 - 3)$, with a 3D. at $Pe = 1$.

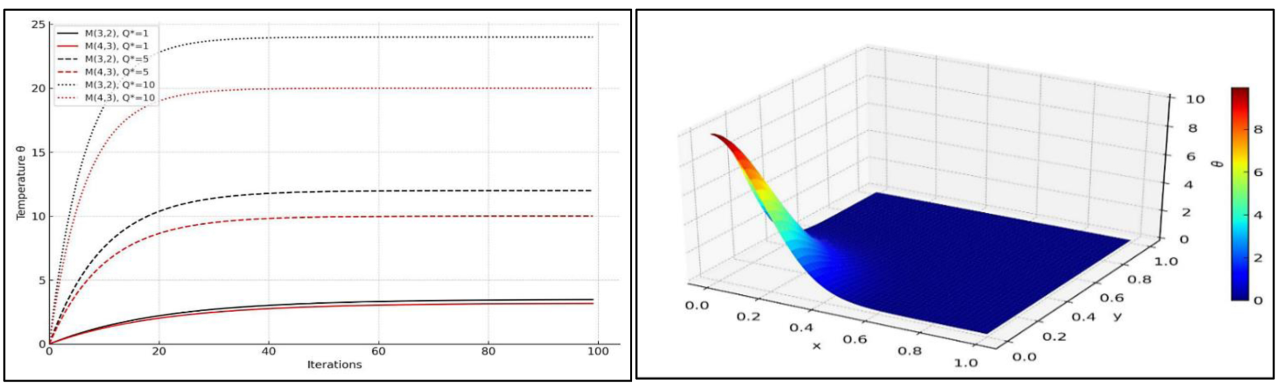

Fig. 7. Effects of the Q^* on the energy equation $Q^* = (1 - 10)$, with a 3D. at $Q^* = 5$.

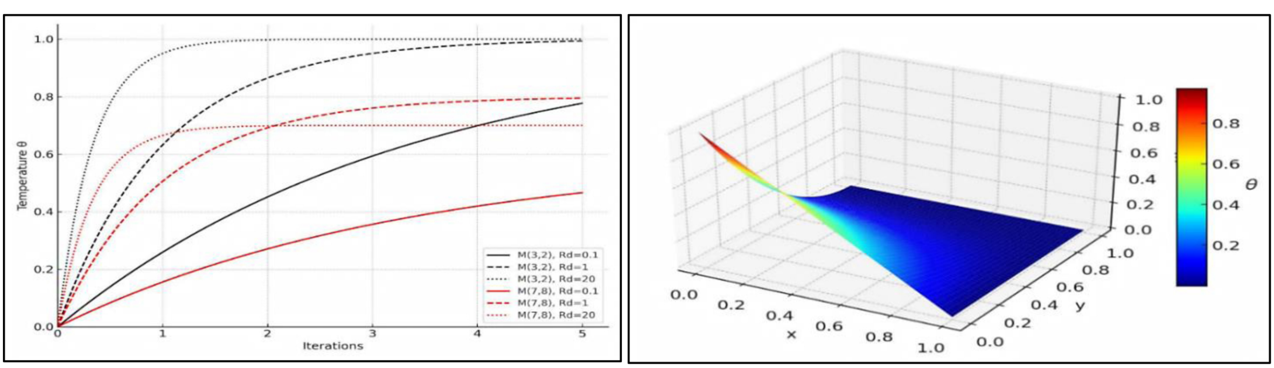

Fig. 8. Effects of the Rd. on the energy equation $Rd = (0.1 - 20)$, with a 3D. at $Rd = 20$.

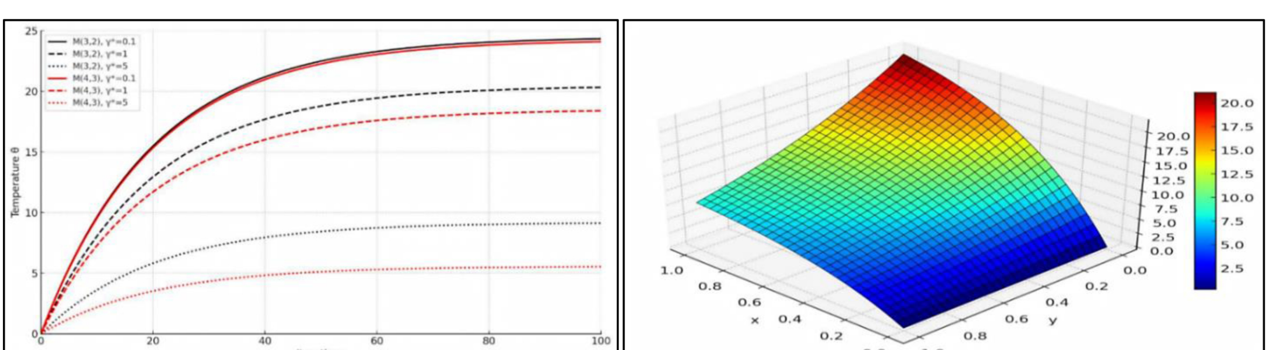

Fig. 9. Effects γ^* on the energy equation $\gamma^* = (0.1 - 5)$, with a 3D. at $\gamma^* = 1$.

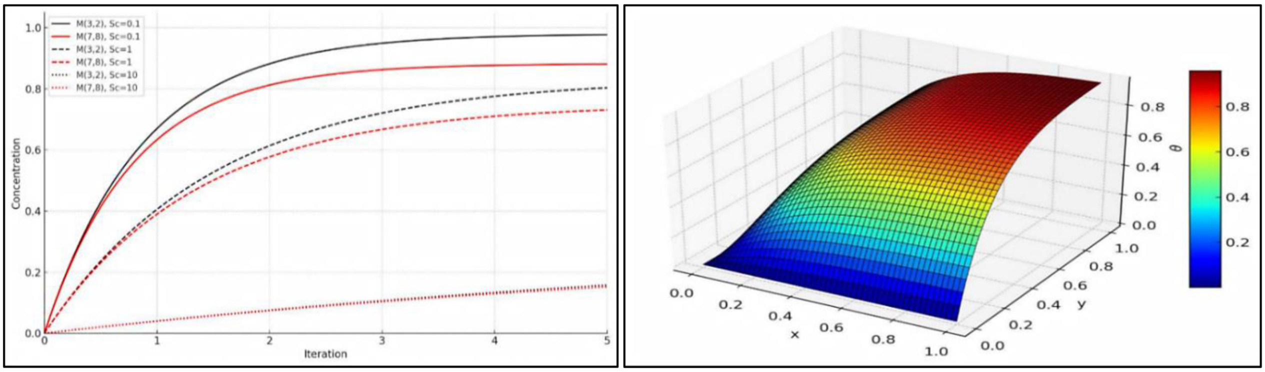

Fig. 10. Effects Sc. on the diffusion equation $Sc = (0.1 - 10)$, with a 3D. at $Sc = 0.1$.

Conclusions

In this section, the numerical results of the studied differential Eqs. (22) to (24) are shown, supported by illustrations (2–10). The stability of flow and the diffusion of heat and mass inside the porous medium depend on the equivalence of the forces of convection, conduction, and diffusion. The lower the Reynolds number, the Grashof number for mass, the Pécletnumber, and the Embedded Radiation, the more stable the system is, as shown in Figs. 2, 3, 6 and 7 by reducing the effect of momentum and thermal buoyancy from the equations of motion and energy. While increasing the Darcy and Grashof number for heat, Radiation effect, and thermal absorption coefficient leads to improving the performance of the thermodynamic system, as shown in Figs. 4, 5, 8 and 9 in both the equations of motion and energy, while getting an increase in concentration and a decrease in mass when the value of Grashof is increased, which negatively affects the stability of the flow, as shown in Fig. 10 in the diffusion equation.

Acknowledgement

The authors extend their sincere thanks to the University of Mosul/College of Education for Pure Sciences for the facilities and support it provided, which contributed effectively to the completion of this work and the improvement of its scientific level.

Authors' declaration

- Conflict of Interest: None.
- We hereby confirm that all the Figures in the manuscript are ours. Furthermore, any Figures and images that are not ours have been included with the necessary permission for re-publication, which is attached to the manuscript.
- No animal studies are present in the manuscript.
- No human studies are present in the manuscript.
- Ethical Approval: The project was approved by the local ethics committee at the University of Mosul.

Authors' contributions statement

S. M. Y. and I. A. designed the study. S. M. Y. and I. A. performed the experiments. S. M. Y. and I. A. performed simulations. S. M. Y. and I. A. expressed and purified all proteins. S. M. Y. and I. A. analyzed the data. S. M. Y. and I. A. wrote the paper with input from all authors.

References

1. Amin MR, Ullah MS, Talukder MMG. Analytical soliton solutions and dynamic behaviors of a fractional nonlinear model in relativistic wave mechanics. AIP Adv. 2025;15(10). https://doi.org/10.1063/5.0299718.

2. Sarojamma G, Sreelakshmi K, Animasaun IL. Numerical study of non-linear thermal radiative heat transfer in a non-Darcy chemically reactive Casson fluid flow. SN Appl. Sci. 2019;1(10):1136. https://doi.org/10.1007/s42452-019-1159-z.
3. Abu Zeid M, Ali KK, Shaalan MA, Raslan KR. Numerical study of thermal radiation and mass transfer effects on free convection flow over a moving vertical porous plate using cubic B-spline collocation method. J Egypt Math. Soc. 2019;27(1):36. https://doi.org/10.1186/s42787-019-0035-8.
4. Liu S, Jiang L, Chong KL, Zhu X, Wan Z-H, Verzicco R, *et al.* From Rayleigh–Bénard convection to porous-media convection: how porosity affects heat transfer and flow structure. J Fluid Mech. 2020;895:A18. http://dx.doi.org/10.1017/jfm.2020.309.
5. Feng X-B, Liu Q, He Y-L. Numerical simulations of convection heat transfer in porous media using a cascaded lattice Boltzmann method. Int J Heat Mass Transf. 2020;151:119410 http://dx.doi.org/10.1016/j.ijheatmasstransfer.2020.119410.
6. Asjad MI, Ikram MD, Akgül A. Analysis of MHD viscous fluid flow through porous medium with novel power law fractional differential operator. Phys Scr. 2020;95(11):115209.
7. Hammodat A, Algwauish G, Al-Obaidi I. The Effects of Electrical Conductivity on Fluid Flow between Two Parallel Plates in a Porous Medioum. Iraqi J Sci. 2021;62(12):4953–4963. http://dx.doi.org/10.24996/ijs.2021.62.12.32.
8. Danish GA, Imran M, Tahir M, Waqas H, Asjad MI, Akgül A, Baleanu D. Effects of non-linear thermal radiation and chemical reaction on time-dependent flow of Williamson nanofluid with combined electrical MHD and activation energy. J Appl Comput Mech. 2021;7(2):546–558. https://doi.org/10.22055/jacm.2020.35122.2568.
9. Ikram MD, Imran MA, Chu YM, Akgül A. MHD flow of a Newtonian fluid in symmetric channel with ABC fractional model containing hybrid nanoparticles. Combinatorial Chemistry & High Throughput Screening. 2022;25(7):1087–1102. https://doi.org/10.2174/1386207324666210412122544.
10. Al-kazzaz RM, Mohammad SA. Effects of Radiation on Free Convection Non-Darcy Flow along Non-isothermal Vertical Wall Embedded in a Porous Medium with Heat Generation. Int Res J Innov Eng Technol. 2022;6(6):99–107. http://dx.doi.org/10.1615/JPorMedia.v17.i3.70.
11. Rahaman MM, Takia H, Hasan MK, Hossain MB, Mia S, Hossen K. Application of Advection Diffusion Equation for Determination of Contaminants in Aqueous Solution: A Mathematical Analysis. Appl Math Phys. 2022;10(1):24–31.
12. Ahmad B, Ahmad MO, Farman M, Akgül A, Riaz MB.Significance of multi-slip condition for inclined MHD nanofluid flow with nonlinear thermal radiation, Dufour and Soret effects, and chemically reactive bioconvection. S Afr J Chem Eng. 2023;43:135–145 https://doi.org/10.1016/j.sajce.2022.10.009.
13. Abbas A, Khan A, Abdeljawad T, Aslam M. Numerical simulation of variable density and magnetohydrodynamics effects on heat generating and dissipating Williamson Sakiadis flow in a porous space: Impact of solar radiation and Joule heating. Heliyon. 2023;9(11):e21726. http://dx.doi.org/10.1016/j.heliyon.2023.e21726.
14. Al-Shammari ISS, Al-Khafajy DGS. Influence of Temperature on The Concentration and thus on the MHD Oscillatory Flow of a Tangent Hyperbolic Fluid Through a Regular Permeable Channel. J Al-Qadisiyah Comput Sci Math. 2024;16(2):36–46. https://doi.org/10.29304/jqcsm.2024.16.21549.
15. Choudhury K, Sharma S. Natural convection MHD mass transfer through an infinite vertical porous plate in the existence of radiation embedded in porous medium. Heat Transf. 2024;53(3):1031–1049. http://dx.doi.org/10.1002/htj.22984.
16. Saleem HD. Heat Transfer of Fluid Flow by Conduction and Convection in Inclined Cavities. Al-Rafidain J Comput Sci Math. 2024;18(2):105–110. http://dx.doi.org/10.33899/csmj.2024.150040.1129.
17. Kumar R, Mehta R, Bhatnagar A, Ozsahin I, Uzun B, Almohsen B, *et al.* Numerical Study of Williamson Fluid Flow over a Stretching Sheet with Newtonian Heating Embedded in a Porous Medium in Presence of Thermal Radiation and Heat Source/Sink. J Nonlinear Math Phys. 2025;32(1):4. http://dx.doi.org/10.1007/s44198-024-00258-1.
18. Brewster MQ. Thermal Radiative Transfer and Properties. New York: John Wiley & Sons; 1992.
19. Nassief AM, Abdulhadi AM. Peristaltic Transport of Non-Newtonian Fluid under Effects of Magnetic Force and Heat Transfer in a Symmetric Channel through a Porous Medium. Baghdad Sci J. 2024;21(4):1339–1354. http://dx.doi.org/10.21123/bsj.2023.7835.
20. Kogan E. Nonlinear Transmission Line: Shock Waves and the Simple Wave Approximation. Mathematics. 2025;13(19):3215. https://doi.org/10.3390/math13193215.
21. Bahmani M, Jalili, B, Jalili P, Mirzaei A, Ganji DD. Effect of variations hollow of octagon porous media on heat and mass transfer. Int J Thermofluids. 2024;21:100576. DOI: https://doi.org/10.1016/j.ijft.2024.100576.
22. Abdulsahib AA, Fadhel FS, Eidi JH. Approximate Solution of Linear Fuzzy Random Ordinary Differential Equations Using Laplace Variational Iteration Method. Iraqi J Sci. 2024;65(2):804–817. https://doi.org/10.24996/ijs.2024.65.2.18.

دراسة عددية لتأثير الإشعاع المدمج على جريان السوائل وانتقال الحرارة في وسط مسامي

شيماء محمد يونس، ايمان العبيدي

قسم الرياضيات، كلية التربية للعلوم الصرفة، جامعة الموصل، الموصل، العراق.

الخلاصة

تهدف هذه الدراسة إلى دراسة نمط التدفق ثنائي الأبعاد للسوائل في وسط موصل محصور بين صفيحتين أفقيتين متوازيتين تحت تأثير الإشعاع المُدمج. يعتمد النموذج الرياضي على معادلات التدفق، بما في ذلك معادلات الاستمرارية، والزخم، والقوة، والانتشار. حُلّت هذه المعادلة عدديًا باستخدام طريقة الفروق المحدودة المحددة (ADE) لدراسة سلوك الانجراف، والحرارة، وانتقال الكتلة تحت التأثيرات الإشعاعية. تركز الدراسة على تأثير المعلمات الرئيسية عديمة الأبعاد، بما في ذلك معامل رينولدز، وعدد دارسي، ومعامل غراشوف، وعدد بيكليت، ومعامل الإشعاع، والإشعاع المُركّب، ومعامل الامتصاص الحراري، على درجة الحرارة وتوزيع الوعي في الوسط المسامي. تشير النتائج إلى أن زيادة الإشعاع المُركّب تُكمّل درجة الحرارة في الطبقة المسامية، بينما يُؤثر معامل دارسي بشكل كبير على سرعة السائل وتوازنه. تم استخدام برنامج MATLAB لإجراء الحل العددي وتصور النتائج، مما يمنح فهمًا واضحًا لسلوك الطفو وانتقال الحرارة والكتلة في الوسائط المسامية تحت تأثيرات الإشعاع الحراري. وتكمن أهمية هذه الدراسة في توضيح الدور المحوري للإشعاع الحراري في تعديل وتحسين خصائص انتقال الحرارة داخل الأوساط المسامية.

الكلمات المفتاحية: طريقة الاتجاهات الصريحة، عدد دراسي، الاشعاع المدمج، معامل الاشعاع، معامل الامتصاص الحراري.